Estuarine, Coastal and Shelf Science 152 (2015) 124–133

Contents lists available at ScienceDirect

Estuarine, Coastal and Shelf Science

journal homepage: www.elsevier.com/locate/ecss

Acoustic backscatter observations with implications for seasonal and vertical migrations of zooplankton and nekton in the Amundsen shelf (Antarctica)

H.S. La [a], H.K. Ha [a, b, *], C.Y. Kang [a], A.K. Wåhlin [c], H.C. Shin [a]

[a] Korea Polar Research Institute, Incheon 406-840, South Korea
[b] Department of Ocean Sciences, Inha University, Incheon 402-751, South Korea
[c] Department of Earth Sciences, University of Gothenburg, Gothenburg, Sweden

ARTICLE INFO

Article history:
Received 15 April 2014
Accepted 15 November 2014
Available online 21 November 2014

Keywords:
ADCP
acoustic backscatter
sea ice
diel vertical migration
Amundsen Sea

ABSTRACT

High-temporal resolution profiles of acoustic backscatter were collected in the Dotson Trough on the Amundsen shelf in the Antarctica, using a bottom-moored, upward-looking acoustic Doppler current profiler (ADCP). This data set was used to examine the impact of seasonal variations in surface solar radiation (SSR), sea ice concentration (SIC), and Circumpolar Deep Water (CDW) thickness on acoustic backscatter in the lower water column (250–540-m depth). A recorded high acoustic backscatter (−75 to −70 dB) at depth >400 m from April to November compared to the rest of the year (−90 to −80 dB) suggests that zooplankton and nekton migrated towards the bottom during winter. The depth of maximum mean volume backscattering strength showed a significant correlation with SSR, SIC and CDW thickness. A daily cycle of vertical migration was also recorded. This varied with changing surface ice conditions. When sea ice cover was low, the acoustic backscatter descended at sunrise, and ascended at sunset. When sea ice cover was high, the daily migration was not pronounced, and the layer of high acoustic backscatter remained near the bottom. This is the first study of seasonal and vertical migration of zooplankton and nekton that has been conducted on the Amundsen Sea shelf, one of the world's most productive areas. The findings provide implications to understand the behavior of zooplankton and nekton below the euphotic zone in the Southern Ocean.

1. Introduction

The acoustic Doppler current profiler (ADCP) is an important tool used to study not only velocity profiles (Schott, 1986; Kaneko et al., 1990; Shin et al., 2006; Kang et al., 2012) but also acoustic backscatter from marine organisms (e.g., zooplankton and nekton) (Flagg and Smith, 1989; Zimmerman and Biggs, 1999; Wade and Heywood, 2001; Lu et al., 2007; Benoit et al., 2008; Geoffroy et al., 2011). The ADCP has helped determine the spatial and temporal distributions of zooplankton in many regions (Plueddemann and Pinkel, 1989; Zhou et al., 1994; Blachowiak-Samolyk et al., 2006; Brierley et al., 2006; van Haren, 2007; Berge et al., 2009; Cisewski et al., 2010; Wallace et al., 2010). Using moored ADCPs, seasonal and inter-annual patterns and diel vertical migration (DVM) of zooplankton have been monitored over long-term periods, providing insight into the possible causes of variation in these factors, which would be unattainable with regular ship-based samplings (van Haren, 2007; Cisewski et al., 2010; Wallace et al., 2010).

Vertical migration is a common behavior exhibited by zooplankton, and it may be caused by predator avoidance (Zaret and Suffern, 1976; Bollens et al., 1992; Fortier et al., 2001), phytoplankton distribution (Thorisson, 2006), and biorhythm (Hays, 2003). It is also reported to be triggered by variations in light intensity (Forward, 1988; Ringelberg, 1995). As vertical migration occurs on diel, seasonal and inter-annual time scales, long-term observational data with high-temporal resolution is needed to study the characteristic patterns of vertical migration over the entire temporal range. Long-term observations can also help understand the effects on vertical migration of environmental changes including global climate change and the cycling of carbon and nutrients (Al-Mutairi and Landry, 2001; Steinberg et al., 2002).

* Corresponding author. Department of Ocean Sciences, Inha University, Incheon 402-751, South Korea.
E-mail addresses: hokyung.ha@gmail.com, hahk@inha.ac.kr (H.K. Ha).

http://dx.doi.org/10.1016/j.ecss.2014.11.020
0272-7714/

Despite many decades of research on vertical migration, our understanding on the role of environmental factors (e.g., light and sea ice) in Polar Oceans is still limited. This is mainly because the harsh weather and sea ice limit the access to areas where long-term observational data is necessary. The lack of such data has impeded our evaluation and prediction of the zooplankton life cycle in Polar Oceans, where sea ice concentration (SIC) might affect vertical migration patterns.

To better understand vertical migration, an ADCP was moored in the Dotson Trough on the Amundsen shelf in Antarctica (Fig. 1). The Amundsen Sea is one of the most productive regions in the Southern Ocean, and extensive phytoplankton blooms have been consistently detected during austral summer via satellite-based ocean color sensors (Arrigo and van Dijken, 2003; Arrigo et al., 2012). This sea is ideal for observing the seasonal variability of acoustic backscatter because of the region's rapid variation in SIC as well as its high productivity. The aim of this study is to provide the assessment of the seasonal and vertical migration of acoustic backscatter as a proxy for abundance/biomass of zooplankton and nekton below the euphotic zone in seasonally ice-covered region. It would have been preferable to have ground-truth data (e.g., by net sampling) to verify the linkage between acoustic backscatter and zooplankton/nekton abundance. Clearly it is not possible to perform continuous net samplings for one year in this region but make the reasonable guess on migrating behaviors for various species. It is convinced that the present acoustic data set could provide implications for the diel and seasonal migration of zooplankton and nekton from one of the most hostile and under-sampled places on Earth.

2. Materials and methods

2.1. Mooring location

The mooring system was installed on the eastern side of the Dotson Trough (72°27.35′S, 116°20.33′W) in the Amundsen Sea during the *Oden* OSO0910 cruise (February 16, 2010), and then recovered during the *Araon* ANA01C cruise (December 25, 2010) (Fig. 1). The Amundsen Sea has been the focus of studies on the accelerated thinning of glaciers caused by warm, salty water beneath the ice shelves (Walker et al., 2007; Arneborg et al., 2012; Pritchard et al., 2012; Wåhlin et al., 2012, 2013; Ha et al., 2014). This warm water mass is derived from Circumpolar Deep Water (CDW; upper boundary was defined by 0 °C isotherm) (Wåhlin et al., 2010; Jacobs et al., 2012), a voluminous water mass found off the continental shelves around Antarctica (Orsi et al., 1995). The Dotson Trough provides a major conduit for the delivery of large volumes of CDW onto the shelf, with the main pathway of CDW inflow along the trough's eastern side (Ha et al., 2014). CDW above 0.6 °C flowed persistently in the Dotson Trough during the sampling period (2010–2012), and its thickness and temperature peaked in late summer and early fall (Wåhlin et al., 2013). The depth-averaged along-trough velocity during this period was about 0.024 m s^{-1} (Wåhlin et al., 2013).

2.2. Data collection

The mooring was equipped with a 150-kHz ADCP (RDI, Workhorse Quartermaster) and an array of five MicroCats measuring conductivity, temperature, and pressure (Seabird, SBE-37) from the

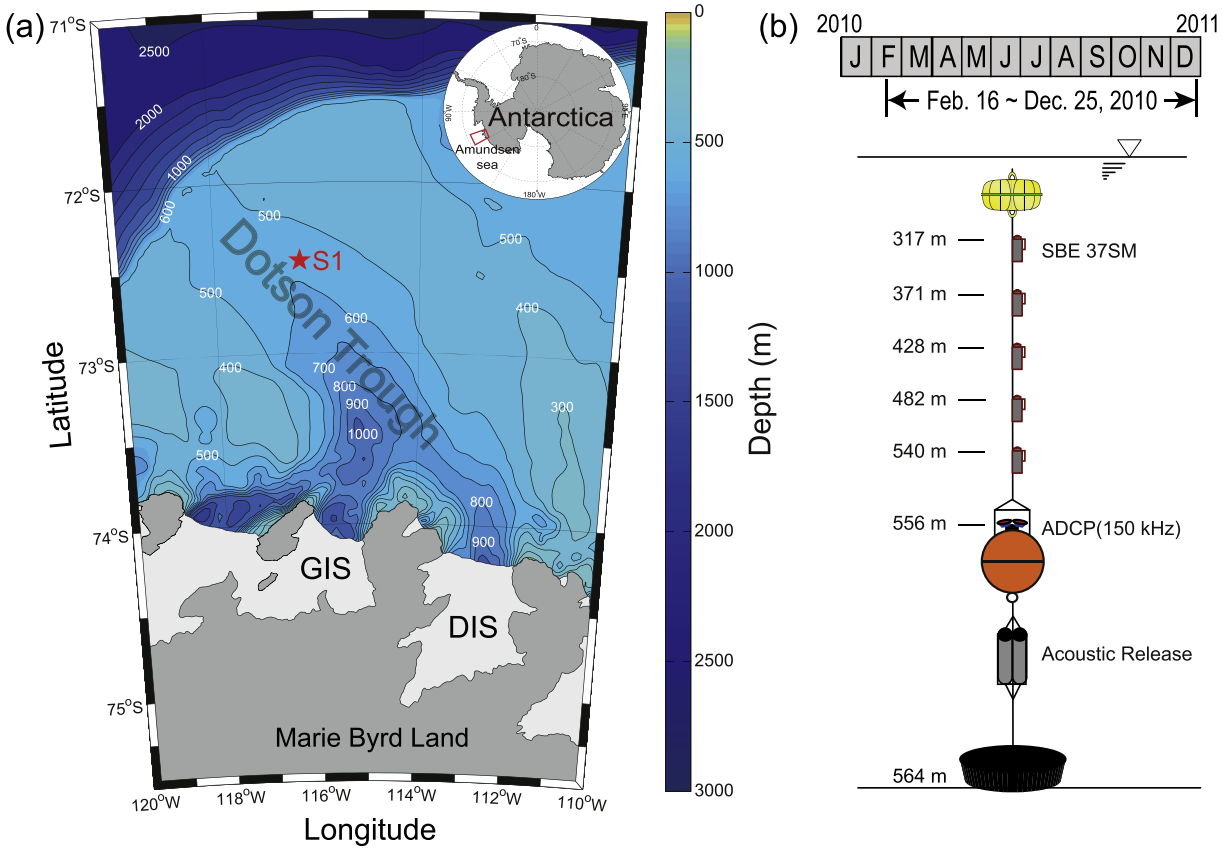

Fig. 1. (a) Map of the study area. The star (S1) indicates the mooring location (72°27.35′S, 116°20.33′W). (b) Design of the mooring system. GIS: Getz Ice Shelf; DIS: Dotson Ice Shelf.

bottom up to 320 m (Fig. 1b). Data collected between March 1 and December 25, 2010 was analyzed to compare the monthly variability of acoustic backscatter. The accuracies of the probes are 0.0003 S m^{-1} for conductivity, 0.002 °C for temperature, and 0.1% of the full depth range for pressure. Temperature and salinity were recorded at 10-min intervals in order to delineate the hydrographic variation in water column.

The ADCP was moored in an upward-looking configuration at a depth of 556 m to estimate the profiles of velocity and acoustic backscatter. The ADCP has 4 transducers which are oriented with a slant angle of 20° off the vertical axis, and it measured 40 bins with an 8-m bin length. The data were acquired ensonifying the water column from 540- to 250-m depth. The sampling interval was set to 5 pings per ensemble every 15 min. The time series of pressure and tilt (pitch and roll) showed that the mooring system did not move much (<1 m in depth and −0.69°/−0.59° in pitch/roll angle) during the entire mooring period. The acoustic backscatter (0–255 counts) recorded by the ADCP was converted to mean volume backscattering strength (MVBS, dB *re* 1 m^{-1}) using the equation presented by Deines (1999).

Sunrise and sunset times at the mooring location were extracted from the astronomical database of the US Naval Observatory (http://aa.usno.navy.mil/). To characterize the seasonal variability of light intensity, the surface solar radiation (SSR, W m^{-2}) data with 6-h interval were retrieved from the National Center for Environmental Prediction/National Center for Atmospheric Research (NCEP/NCAR) reanalysis. A radiation sensor (LI-400, LI-COR Corp.) was used to test the correlation between the reanalysis data of SSR and *in-situ* light intensity (μmol s^{-1} m^{-2}). We conducted field measurements of light intensity at 15-min interval in the Amundsen Sea during the period of March 1–10, 2012. Results (not shown here) demonstrate a good correlation between the reanalysis data of SSR and *in-situ* light intensity ($r^2 = 0.80$, $n = 40$).

We retrieved SIC data from the European Centre for Medium-Range Weather Forecasts (ECMWF) ERA-Interim reanalysis. SIC was based on analysis received daily with global coverage (0.75° × 0.75°) from the Operational Sea Surface Temperature and Sea Ice Analysis.

Chl-*a* (mg m^{-3}) was 8-day averaged based on the daily composite of Moderate Resolution Imaging Spectroradiometer (MODIS) Aqua Level 3 data (4-km resolution) around the mooring station (72°S–73° 30′S, 118°W–112°W).

3. Results

3.1. Seasonal variability of acoustic backscatter and environmental factors

The representative sea ice distributions were captured from late summer (March 3) and late winter (September 18) in 2010, respectively (Fig. 2). Both images are from MODIS Aqua (1-km resolution) obtained from the NASA Earth Observing System Data and Information System. A coastal polynya is visible along the ice shelf from 100 to 120°W, expanding northward up to 71°S during March (Fig. 2a). In September, the Amundsen Sea was completely covered with sea ice (Fig. 2b).

SSR gradually decreased from March to May, remained near zero in May–August, and then increased from August onward (Fig. 3a). The mooring position was covered by high SIC between April and December, when the SSR was comparatively low (Fig. 3b). Water temperature profiles indicated the existence of CDW, ranging from 0 to 1.5 °C at depths of 420–540 m over the entire time period (Fig. 3c). The thickness of the CDW layer increased and its inflow became strong during late summer and fall, whereas it decreased and its inflow became weak during late winter and spring (Wåhlin et al., 2013; Ha et al., 2014). A high current speed (>0.1 m s^{-1}) was observed before July, when the CDW layer was comparatively thick. After that, the inflow speed decreased to 0.05 m s^{-1} with decreasing CDW thickness (Fig. 3d). High levels (>−75 dB) of MVBS mainly occurred below 400 m between mid-April and mid-November. During the rest of the year (December to March), relatively low acoustic backscatter (−90 to −80 dB) was observed over the water column (Fig. 3e). The depth of maximum MVBS (D_{MVBS}, 3-day moving average) deepened toward the bottom between March and May, and lifted to a depth (~250 m) between mid-November and December (Fig. 3e).

Seasonal changes in acoustic backscatter patterns accompanying variations in SSR, SIC and CDW thickness were clearly visible in monthly averaged values (Table 1). SSR decreased from March (78.1 W m^{-2}) to July (0 W m^{-2}), and then rapidly increased again in

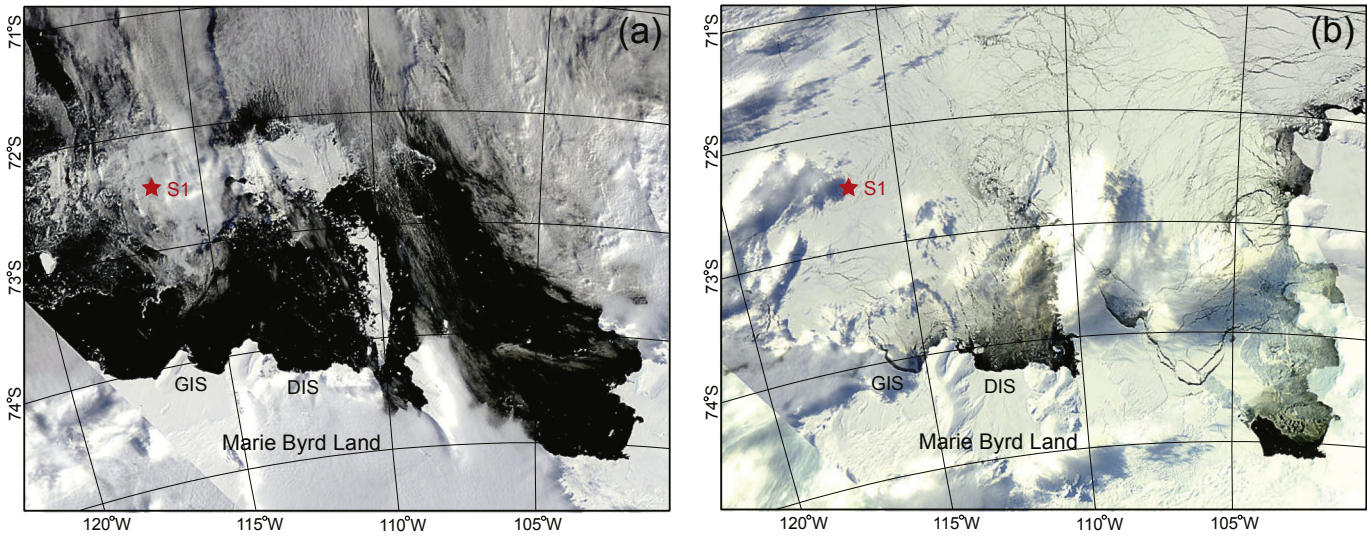

Fig. 2. Sea ice distribution captured by MODIS on NASA's Aqua satellite on: (a) March 9 and (b) September 11, 2010. The star (S1) indicates the mooring location. GIS: Getz Ice Shelf; DIS: Dotson Ice Shelf.

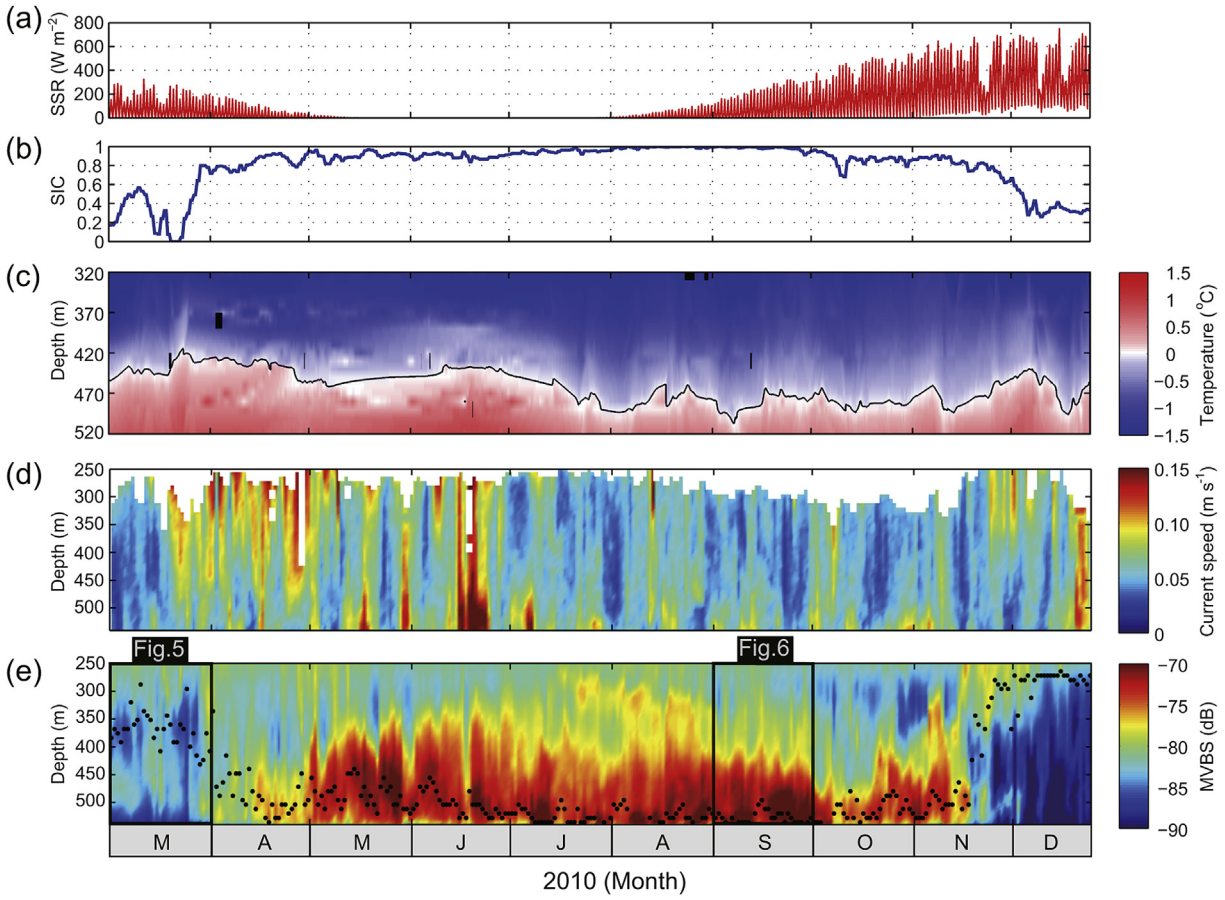

Fig. 3. Seasonal variability in acoustic backscatter and related environmental parameters: (a) SSR; (b) SIC; (c) potential temperature; (d) current speed; and (e) MVBS. Black line in (c) represents the isotherm of 0 °C showing the upper boundary of CDW. Black and white areas in (c) and (d) indicate the data removed for quality control, respectively. Black dots in (e) indicate D_{MVBS}.

Table 1
Monthly averages of SSR, SIC, CDW thickness, MVBS and D_{MVBS} during the mooring period.

	Mar.	Apr.	May	Jun.	Jul.	Aug.	Sep.	Oct.	Nov.	Dec.
SSR (W m^{-2})	78.1	27.2	1.2	0.0	0.0	14.4	79.5	179.7	272.9	321.8
SIC	0.3	0.8	0.9	0.9	0.9	1.0	1.0	0.9	0.8	0.4
CDW thickness (m)	127	129	110	122	99	86	82	83	91	102
Depth-integrated (250–540 m) MVBS (dB)	−82.4	−79.7	−75.1	−75.2	−75.8	−74.9	−74.9	−78.1	−79.2	−85.7
D_{MVBS} (m)	335.7	471.7	471.7	487.7	511.7	511.7	519.7	503.7	415.7	255.7

September simultaneously with the decrease in SIC, attaining a maximum of about 321.8 W m^{-2} in December. SIC steeply increased from March to August, and decreased after September, as SSR increased. The CDW thickness varied seasonally over the year. Thickness generally decreased between April and September, and then increased again in October. The maximum was about 129 m in April, and the minimum was about 82 m in September. A high intensity of depth-integrated (250–540 m) MVBS was observed between May and September; it increased from March (−82.4 dB) to May (−75.1 dB) and declined from September. The minimum value (−85.7 dB) was observed during December, when SSR was high and SIC was low. D_{MVBS} rapidly deepened from 335.7 to 471.7 m between March and April, and lifted from 415.7 to 255.7 m between November and December.

SSR and SIC were 3-day averaged to examine the impact of each variable on D_{MVBS} (Fig. 4). The observed seasonal pattern of D_{MVBS} was significantly correlated with SSR, SIC and CDW thickness. Variance inflation factors of SSR, SIC and CDW thickness were less than 2, which imply that there was no multicollinearity between these environmental variables. Instead, a multiple linear regression analysis suggested that increases in SIC and decreases in both SSR and CDW thickness predict D_{MVBS} ($D_{MVBS} = 374.15 + 218.62 \cdot SIC - 0.24 \cdot SSR - 0.64 \cdot CDW$, $r^2 = 0.79$, $n = 300$, $p < 0.001$).

3.2. Daily patterns for austral summer and winter seasons

Two time periods, late summer (March) and late winter (September), were selected to investigate the variability in acoustic backscatter associated with different SIC conditions (Fig. 3). These two months were representative time windows, exhibiting high differences in SIC, but with similar light intensity. During late summer, mean SSR and SIC were about 77.4 W m^{-2} and 0.4, respectively (Fig. 5a and b). The upper boundary of the CDW varied in depths of 420–460 m (mean: 440 m) (Fig. 5c). The current speed

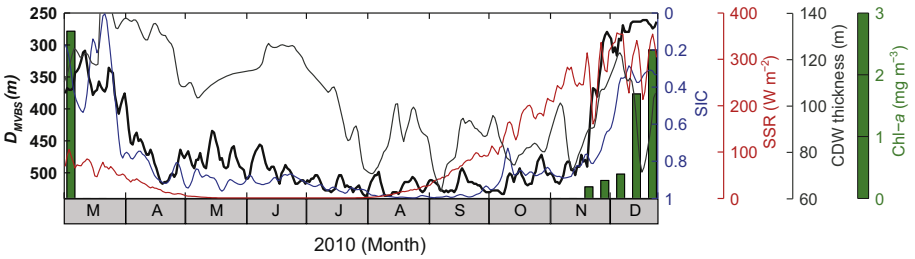

Fig. 4. Relationships among SSR (red line), SIC (blue line), CDW thickness (light gray line), Chl-*a* concentration (green bar), and D_{MVBS} (thick black line). SSR, SIC, CDW thickness and MVBS were 3-day moving averaged to remove undesirable noise. Chl-*a* was 8-day averaged with MODIS Aqua Level 3 data (4-km resolution). Note that the satellite-derived Chl-*a* was not available between early March and December due to high SIC. (For interpretation of the references to color in this figure legend, the reader is referred to the web version of this article.)

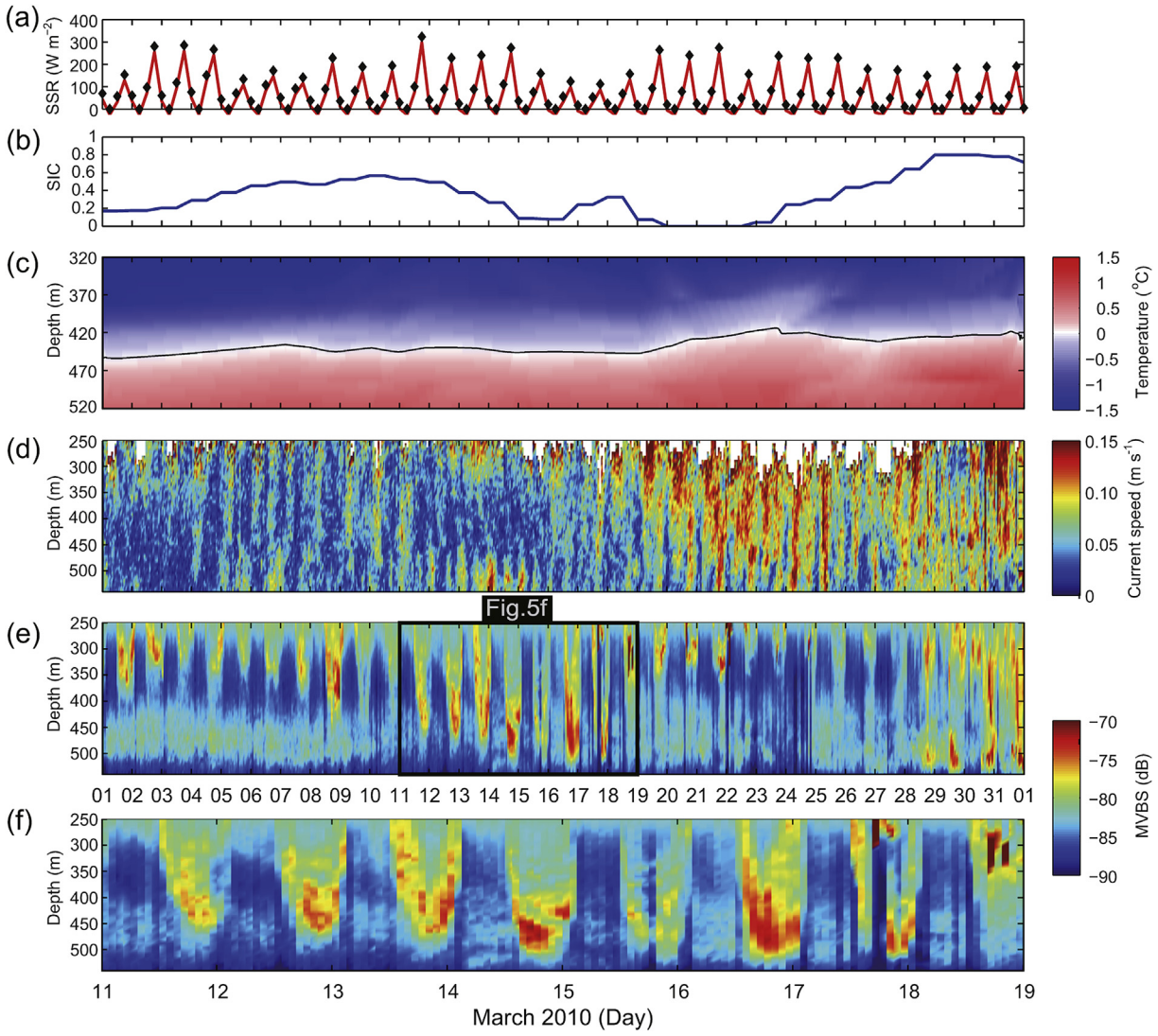

Fig. 5. Temporal variability in acoustic backscatter and related environmental parameters during late summer (March 2010): (a) SSR; (b) SIC; (c) potential temperature; (d) current speed; (e) MVBS; and (f) MVBS enlarged for the time window of March 11–19. Black line in (c) represents the isotherm of 0 °C showing the upper boundary of CDW. White area in (d) indicates the data removed for quality control.

was <0.08 m s^{-1} before March 19, but >0.13 m s^{-1} after that (Fig. 5d). A daily pattern is evident in the vertical distribution of MVBS between 250 and 540 m throughout the diel cycle, with alternating upward and downward movement associated with variations in SSR (Fig. 5e). Although daily patterns were observed in depths of 250–540 m before March 19, after this date, downward movement was sustained only at around 350 m and with an irregular diel pattern. This might be due to the higher current speed (~0.12 m s^{-1}). Close examination of the daily pattern (Fig. 5f) indicates that acoustic backscatter started to descend toward the

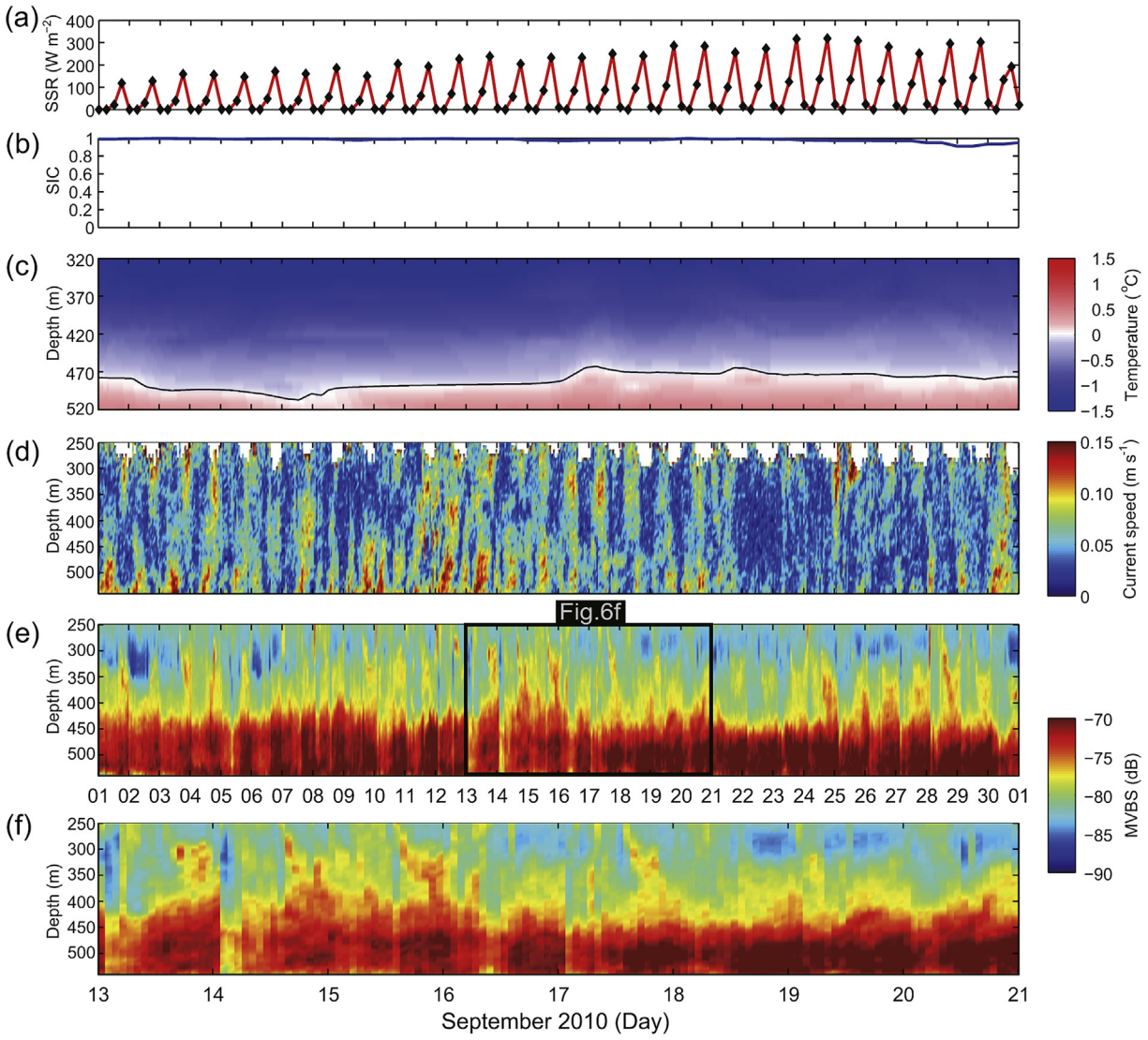

Fig. 6. Temporal variability in acoustic backscatter and related environmental parameters during late winter (September 2010): (a) SSR; (b) SIC; (c) potential temperature; (d) current speed; (e) MVBS; and (f) MVBS enlarged for September 13–21. Black line in (c) represents the isotherm of 0 °C showing the upper boundary of CDW. White area in (d) indicates the data removed for quality control.

bottom when SSR started to increase. The onset of upward movements precisely matched low SSR values. MVBS was high (>−80 dB) in the lower part (below 400 m) of daily pattern, while it was low (<-80 dB) in the upper part (250–300 m).

Acoustic backscatter and environmental data collected in late winter (Fig. 6) were quite different from those collected in late summer, except for light intensity; the average SSR was similar to late summer, while average SIC and CDW thickness were only 30 and 60% of these values during late summer, respectively (Table 1). Even if the mooring was covered with sea ice, the average SSR was 79 W m^{-1} (varying 0–300 W m^{-1}), which is similar to late summer (Fig. 6a). The mooring position was covered with high SIC (>0.9) during late winter, while SIC was much more variable (between 0 and 0.8) during late summer (Fig. 6b). During late winter, the mean depth of CDW fell to 480 m (Fig. 6c), indicating a significant deepening of the upper boundary of CDW, compared with late summer. The variation in current speed was also smaller than that during late summer, being in the range of 0–0.15 m s^{-1}. High current speeds (>0.13 m s^{-1}) were only observed near the bottom and in the upper part (>350 m) of the water column (Fig. 6d). Interestingly, no clear signature in the diel pattern was observed in the vertical distribution of MVBS in depths of 250–540 m (Fig. 6e and f). High MVBS (>−75 dB), which was about 5 dB higher than in late summer, was observed at comparatively constant depths below 400 m.

3.3. Diel variability of acoustic backscatter

MVBS was ensemble averaged for March 1–15 and September 1–15 to compare the diel cycle of acoustic backscatter between late summer and winter (Fig. 7). During the period of March 1–15, sunrise and sunset occurred between 12:57–13:31 UTC (hereafter all times indicate UTC) and 02:18–02:55, respectively. DVM was clearly present in depths of 300–500 m, between 12:00 and 03:00 (Fig. 7a). Downward movement began around sunrise at 12:00, and reached the bottom around 15:00; ascent occurred around sunset after 00:00. The duration of DVM was similar to the sunlight daily cycle. During the migration period, MVBS was mainly in the range of −80 to −77 dB across the whole ADCP range, which is about 3–6 dB higher than MVBS during other periods. Current speed

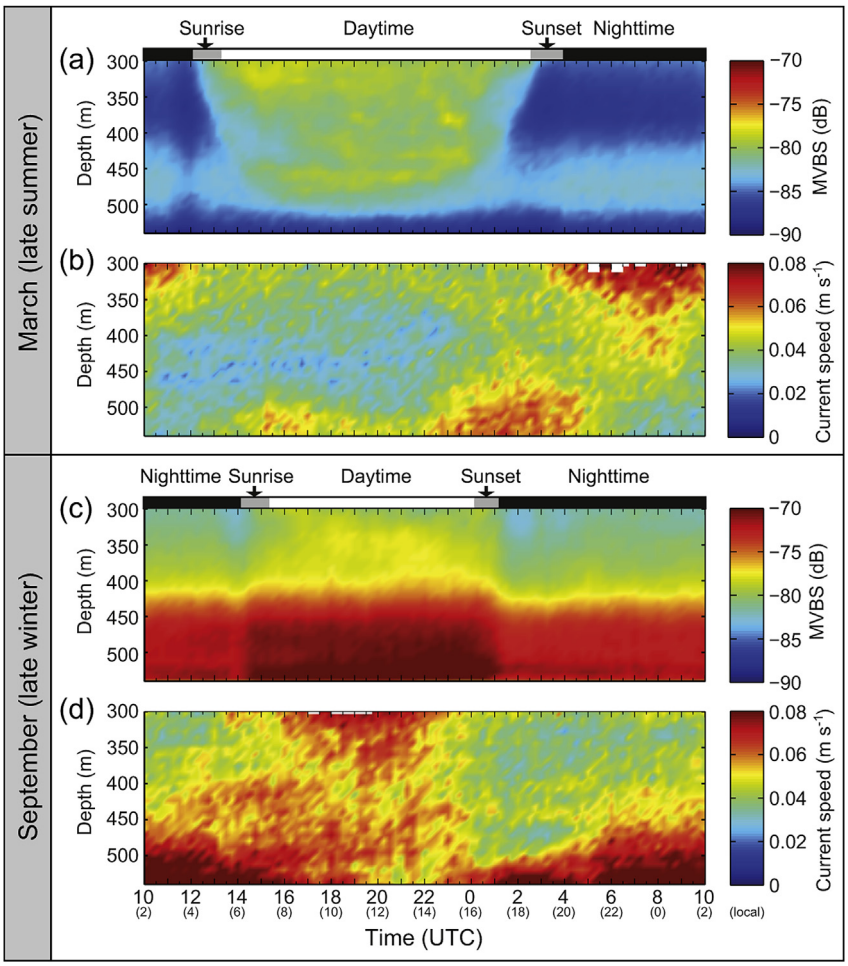

Fig. 7. Mean diel variability of (a) MVBS and (b) current speed during late summer (March 1–15). Mean diel variability of (c) MVBS and (d) current speed during late winter (September 1–15). Note that the local time is 8 h earlier than UTC.

varied in the range of 0.02–0.05 m s^{-1} between sunrise and sunset. High current speeds of >0.07 m s^{-1} were mainly observed in depths of 300–370 m between 04:00 and 10:00, when the low MVBS of <−85 dB was observed in depths of 300–400 m (Fig. 7b). The clear diel pattern captured was associated with low current speed.

During the first half of September (1st–15th), sunrise and sunset occurred between 13:40–14:17 and 01:03–01:35 with about 1-h variation, respectively. The time series of MVBS exhibited a clearly different DVM pattern in late summer (Fig. 7c). MVBS increased with depth. The maximum MVBS (−70 dB) occurred near the bottom between sunrise and sunset, while the minimum MVBS (−83 dB) occurred around 300 m at 14:00–02:00. Higher MVBS values were observed throughout the whole water column in winter, and the maximum was about 7 dB higher than that in late summer. High current speeds (>0.07 m s^{-1}) were observed at most depths during late winter, whereas they were only seen near surface in late summer (Fig. 7d).

4. Discussion

DVM is a widespread behavior shown by arthropods and other invertebrates such as salps and pteropods (Hunt et al., 2008). In particular, it is a common behavior for crustaceans, and frequently observed in euphausiids (Nordhausen, 1994; Siegel et al., 2004), amphipods (Everson and Ward, 1980), and copepods (Atkinson et al., 1992). Unfortunately, from our data, it is not possible to identify the migrating species, as *in-situ* biological samples were not collected due to the harsh weather.

However, the echograms of scientific echo sounder (EK60, Simrad) collected at the mooring station between 01:30 and 03:40 of March 3, 2012 show a deep backscattering layer within 250–350-m depth (Fig. 8a and b). The frequency response ($MVBS_{120-38\ kHz}$) from the backscattering layers at depths of 250–350 m shows a window of 6–18 dB (Fig. 8c). A 120–38-kHz two-frequency ($MVBS_{120-38\ kHz}$) dB window identification technique was used to identify DVM, as it is frequently applied in acoustics for zooplankton identification (Madureira et al., 1993). A negative dB window at $MVBS_{120-38\ kHz}$ is indicative of scattering from organisms containing gas bladders such as siphonophores (Stanton et al., 1998) or fish with swim bladders such as myctophids (Godo et al., 2009). The 6–18-dB window in this study is applicable for zooplankton because $MVBS_{120-38\ kHz}$ window of *Euphausia superba* was described with 2–16 dB for the Southern Ocean in the CCAMLR 2000 survey (Hewitt et al., 2004), and that of *Euphausia crystallorophias* was reported with 6–18 dB in the Amundsen Sea coastal polynya (La et al., 2015). It is also increasingly recognized that *E. crystallorophias* visit the seafloor to feed (Schmidt et al., 2011), and have been identified from epibenthic sledge samples in the Amundsen Sea (Angus Atkinson, Plymouth Marine Laboratory, personal communication) during summer. Thus, one possible species during summer that can produce the backscattering pattern for DVM is *E. crystallorophias*.

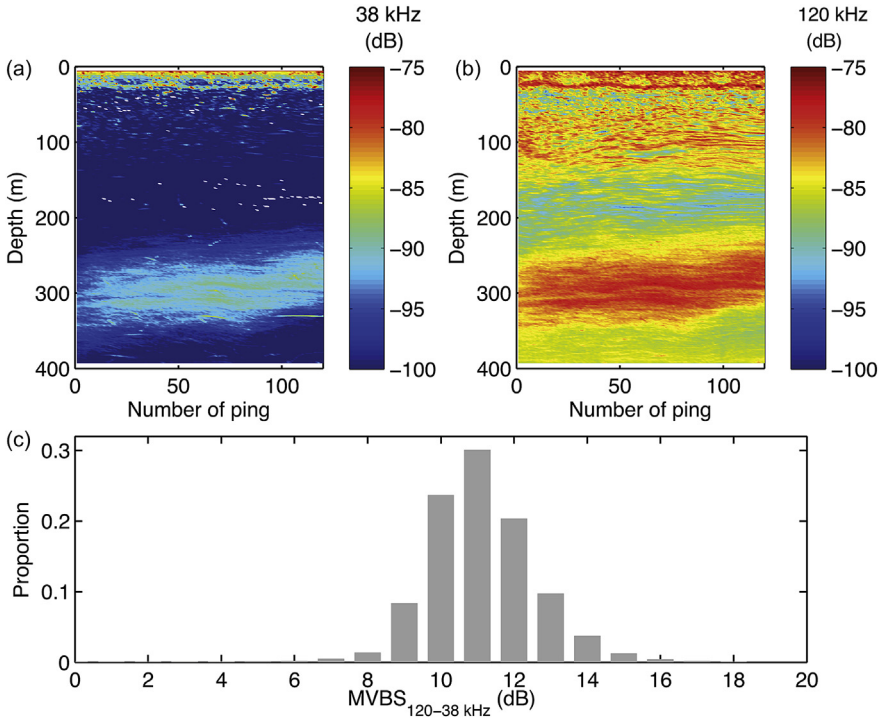

Fig. 8. Echograms recorded at sound frequencies of (a) 38 kHz and (b) 120 kHz on March 3, 2012. (c) $MVBS_{120-38\ kHz}$ dB window. White area in (a) indicates the removed noise data.

The DVM pattern was identified by acoustic backscatter below euphotic zone (20–75 m) (Lee et al., 2012). When SIC was low (March), a clear daily pattern of acoustic backscatter occurred over the ADCP sensing range with the sunlight daily cycle. In contrast, acoustic backscatter remained high near the bottom during high SIC period (September). This pattern very much resembles the general vertical migrations of zooplankton, in which zooplankton ascend to a shallower depth around dusk, and descend around dawn (Roe, 1974; Forward, 1988; Haney, 1988; Ringelberg, 1995; Thomson and Allen, 2000; Cisewski et al., 2010). During the period that food resources are depleted (e.g., austral winter), zooplankton is genetically adapted with body reserves and a state of metabolic depression (Nicol, 2006). Krill overwintering strategies might vary in different habitats but if available, krill will feed efficiently on the seabed detritus because the seabed is rich in organic matters (Smith and Demaster, 2008).

In the seasonally ice-covered region of the Amundsen shelf, the vertical distribution of zooplankton and nekton (indicated by acoustic backscatter) exhibited distinct seasonality, associated with SSR, SIC and CDW thickness (Fig. 4). D_{MVBS} showed a similar pattern to the temporal evolution of the surface phytoplankton biomass, moving to the upper layer between mid-November and December. During the spring and summer, zooplankton is generally distributed in the euphotic zone feeding on the surface phytoplankton and it will go deeper after spring and summer blooms (Lee et al., 2006). The DVM of zooplankton may not closely trace phytoplankton due to slow sinking speed of phytoplankton. However, the availability of phytoplankton may trigger seasonal variability in DVM as the vertical migration of zooplankton is affected by food availability as well as predation by other zooplankton species (Atkinson et al., 1999). There is rich biological production in the ice habitat that can further affect the zooplankton migration. The food availability at the surface may considerably impact the seasonal variability of DVM near the bottom in the seasonal sea ice region, although our data can only indicate the limited vertical pattern of zooplankton below the euphotic depth in the ocean.

Light intensity has been generally accepted as one of the main factors controlling vertical migration of zooplankton (Boden and Kampa, 1967; Ringelberg, 1995; Frank and Widder, 1997). The presence of sea ice could inhibit DVM by blocking the sunlight or by causing diurnal fluctuations in the food web. SIC can reduce the penetration of solar radiation into the ocean by 15–90% (Grenfell and Maykut, 1977). Shading by phytoplankton patches (Isaacs et al., 1974; Andersen et al., 1998) and ice algae (Perovich et al., 1998) can further reduce light penetration. Blachowiak-Samolyk et al. (2006) reported that synchronized DVM was absent during summer in the Arctic. Cottier et al. (2006), however, identified an unsynchronized migration pattern during the Arctic summer, in which zooplankton migrated up and down the water column in an uncoordinated manner. This vertical migration was occasionally linked to the background level of light intensity less than half of the minimum detection level of human eyes (Berge et al., 2009). At subtropical latitudes, the maximum depth of sunlight penetration, which affects DVM near the bottom, was estimated to be about 700 m (Kampa, 1970). Acoustic backscatter observed below 1200 m (e.g., Plueddemann and Pinkel, 1989; van Haren, 2007) has demonstrated that zooplankton migrate vertically even at these depths, where light intensity is below visible levels. Our results showed distinctively different DVM patterns at 250–540-m depths between low and high SIC periods. It appears that sea ice might block out the detectable light intensity, causing a different DVM pattern below intermediate depths (>250 m). It remains for further studies to determine how sea ice might modify the nature and extent of vertical migration of zooplankton in the deep sea.

The vertical distribution of zooplankton during winter is still poorly understood because data in the ice-covered region are scarce due to logistical constraints. The MVBS measured during late winter, indicating a constant presence close to the bottom and no vertical migration, is also possibly caused by euphausiid, copepods, and nekton. During late winter/early spring, older stages of Antarctic copepods *Calanoides actus* and *Calanus propinquus* were observed below 500 m while they were concentrated above 200 m

in summer (Schnack-Schiel et al., 1991). The seabed detritus may be a possible food source, leading to an overall deeper distribution of krill during winter (Zhou et al., 1994; Lawson et al., 2008). *Euphausia crystallorophias* and *Calanus* sp. store wax esters as a dominant storage lipid, which allow diapausing them to be neutrally buoyant in cold deep waters and to avoid spending energy to remain (Kattner and Hagen, 1998; Lee et al., 2006). Diapausing zooplankton enters deep water after feeding on phytoplankton during spring/summer blooms or at the end of upwelling periods (Lee et al., 2006). *Pleuragramma antarcticum* (silverfish) and *Dissostichus mawsoni* (toothfish) are found under the ice of the Ross Sea (Fuiman et al., 2002): silverfish is the most abundant fish in the shelf areas of the Southern Ocean (Dewitt, 1970; Hubold, 1985), and is a key link between plankton and the community of top predators (La Mesa et al., 2004; Smith Jr. et al., 2007). Benoit et al. (2008) and Geoffroy et al. (2011) observed similar deep aggregations of fish (polar cod) in the ice-covered region Arctic Ocean. Unfortunately, little is known about zooplankton and fish distributions during winter, especially in the case of those species living below the heavy pack ice and shore-fast ice of the Amundsen Sea. In future studies, *in-situ* biological net sampling and multi-frequency acoustic survey must be conducted to identify and characterize the provenance of the acoustic backscatter associated with DVM.

5. Conclusions

High-temporal resolution profiles of ADCP backscatter were collected to investigate their seasonal variability under various conditions. The main conclusions drawn from this study can be summarized as follows:

(1) From April to November, relatively high acoustic backscatter (−75 to −70 dB) was found close to the bottom (>400 m), whereas from December to March, low acoustic backscatter (−90 to −80 dB) was observed from 250 to 540 m;
(2) The seasonal cycle of acoustic backscatter was closely related to SSR, SIC and CDW thickness. D_{MVBS} was significantly correlated with these three environmental factors ($r^2 = 0.79$, $p < 0.001$). High MVBS near the bottom (>400 m) during low SSR and high SIC suggests that reduced food availability at the surface might cause the downward vertical migration;
(3) The diel cycle of acoustic backscatter showed a distinctive DVM pattern depending on both light and sea ice. When SIC was low, a typical DVM pattern tracking the sunlight daily cycle (descent at sunrise and ascent at sunset) was observed, and acoustic backscatter was observed through the entire water column. When SIC was high, DVM remained near the bottom with high MVBS. Light is the primary factor that causes a diel cycle in the vertical migration, but sea ice likely blocks out the detectable light intensity for DVM near the bottom seasonally during high SIC periods;
(4) The time series of acoustic backscatter enabled the analysis of MVBS, which exhibits the behavior expected for zooplankton (in summer) and nekton (seasonal migration) biomass. Although specific zooplankton or nekton species could not be identified, it is possible that *Euphausia crystallorophias* (which gives a similar $MVBS_{120-38\ kHz}$ window and migrates in a similar pattern to that observed) may have been present.

Acknowledgments

This work was supported by the K-Polar Program (PP13020 and PP14020) of KOPRI. In the stage of developing signal conversion algorithm, HKH was supported by the Polar Academic Program (PD14010) of KOPRI and Inha University Research Grant (INHA-49278). It was also supported by the Swedish Research Council (Grant number 2013-5273). The authors are deeply indebted to the captains and crews of the IBRVs *Araon* and *Oden* for professional support during the Amundsen expeditions. The authors also thank to J. Park and S.I. Kim for support and helpful comments on the satellite-based chlorophyll and sea ice data.

References

Al-Mutairi, H., Landry, M.R., 2001. Active export of carbon and nitrogen at station ALOHA by diel migrant zooplankton. Deep-Sea Res. II 48, 2083–2103.
Andersen, V., Francois, F., Sardou, J., Picheral, M., Scotto, M., Nival, P., 1998. Vertical distributions of macroplankton and micronekton in the Ligurian and Tyrrhenian Seas (northwestern Mediterranean). Oceanol. Acta 21, 655–676.
Arneborg, L., Wåhlin, A., Björk, G., Liljeblad, B., Orsi, A., 2012. Persistent inflow of warm water through a submarine trough on the central Amundsen Shelf. Nat. Geosci. 5, 876–880. http://dx.doi.org/10.1038/ngeo1644.
Arrigo, K.R., Lowry, K.E., van Dijken, G.L., 2012. Annual changes in sea ice and phytoplankton in polynyas of the Amundsen Sea, Antarctica. Deep-Sea Res. II 71–76, 5–15.
Arrigo, K.R., van Dijken, G.L., 2003. Phytoplankton dynamics within 37 Antarctic coastal polynya systems. J. Geophys. Res. 108 (C8), 3271. http://dx.doi.org/10.1029/2002 JC001739.
Atkinson, A., Ward, P., Hill, A., Brierley, A.S., Cripps, G.C., 1999. Krill-copepod interactions at South Georgia, Antarctica, II. *Euphausia superba* as a major control on copepod abundance. Mar. Ecol. Prog. Ser. 176, 63–79.
Atkinson, A., Ward, P., Williams, R., Poulet, S.A., 1992. Diel vertical migration and feeding of copepods at an oceanic site near South Georgia. Mar. Biol. 113, 583–593.
Benoit, D., Simard, Y., Fortier, L., 2008. Hydro-acoustic detection of large winter aggregations of Arctic cod (*Boreogadus saida*) at depth in ice-covered Franklin Bay (Beaufort Sea). J. Geophys. Res. 113 (C06), S90.
Berge, J., Cottier, F., Last, K.S., Varpe, O., Leu, E., Soreide, J., Eiane, K., Falk-Petersen, S., Willis, K., Nygard, H., Vogedes, D., Griffiths, C., Johnsen, G., Lorentzen, D., Brierley, A.S., 2009. Diel vertical migration of Arctic zooplankton during the polar night. Biol. Lett. 5, 69–72.
Blachowiak-Samolyk, K., Kwasniewski, S., Richardson, K., Dmoch, K., Hansen, E., Hop, H., Falk-Petersen, S., Mouritsen, L.T., 2006. Arctic zooplankton do not perform diel vertical migration (DVM) during periods of midnight sun. Mar. Ecol. Prog. Ser. 308, 101–116.
Boden, B.P., Kampa, E.M., 1967. The influence of natural light on the vertical migrations of an animal community in the sea. Symp. Zool. Soc. Lond. 19, 15–26.
Bollens, S.M., Frost, B.W., Thoreson, D.S., Watts, S.J., 1992. Diel vertical migration in zooplankton: field evidence in support of the predator avoidance hypothesis. Hydrobiologia 234, 33–39.
Brierley, A.S., Saunders, R.A., Bone, D.G., Murphy, E.J., Enderlein, P., Conti, S.G., Demer, D.A., 2006. Use of moored acoustic instruments to measure short-term variability in abundance of Antarctic krill. Limnol. Oceanogr. Methods 4, 18–29.
Cisewski, B., Strass, V.H., Rhein, M., Kragefsky, S., 2010. Seasonal variation of diel vertical migration of zooplankton backscatter time series data in the Lazarev Sea, Antarctica. Deep-Sea Res. 57, 78–94.
Cottier, F.R., Tarling, G.A., Wold, A., Falk-Petersen, S., 2006. Unsynchronized and synchronized vertical migration of zooplankton in a high Arctic fjord. Limnol. Oceanogr. 51, 2586–2599.
Deines, K.L., 1999. Backscatter estimation using broadband acoustic Doppler Current Profilers. In: Proceedings of the 6th IEEE Working Conference on Current Measurement. San Diego, CA, pp. 249–253.
Dewitt, H.H., 1970. The character of the midwater fish fauna of the Ross Sea, Antarctica. In: Holgate, M.W. (Ed.), Antarctic Ecology, vol. 1. Academic Press, London, pp. 305–314.
Everson, I., Ward, P., 1980. Aspects of Scotia sea zooplankton. Biol. J. Linn. Soc. 14, 93–101.
Flagg, C.N., Smith, S.L., 1989. On the use of the acoustic Doppler current profiler to measure zooplankton abundance. Deep-Sea Res. 36 (3), 455–474.
Fortier, M., Fortier, L., Hattori, H., Saito, H., Legendre, L., 2001. Visual predators and the diel vertical migration of copepods under Arctic sea ice during the midnight sun. J. Plankton Res. 23, 1263–1278.
Forward, R.B., 1988. Diel vertical migration: zooplankton photobiology and behaviour. Oceanogr. Mar. Biol. Annu. Rev. 26, 361–396.
Frank, T.M., Widder, E.A., 1997. The correlation of downwelling irradiance and staggered vertical migration patterns of zooplankton in Wilkinson Basin, Gulf of Maine. J. Plankton Res. 19, 1975–1991.
Fuiman, L.A., Davis, R.W., Williams, T.M., 2002. Behavior of midwater fishes under the Antarctic ice: observations by a predator. Mar. Biol. 140, 815–822.
Geoffroy, M., Robert, D., Darnis, G., Fortier, L., 2011. The aggregation of polar cod (Boreogadus saida) in the deep Atlantic layer of ice-covered Amundsen Gulf (Beaufort Sea) in winter. Polar Biol. 34, 1959–1971.
Godo, O.R., Patel, R., Pedersen, G., 2009. Diel migration and swimbladder resonance of small fish: some implications for analyses of multifrequency echo data. ICES J. Mar. Sci. 66, 1143–1148.

Grenfell, T.C., Maykut, G.A., 1977. The optical properties of ice and snow in the Arctic Basin. J. Glaciol. 18, 445–463.
Ha, H.K., Wåhlin, A.K., Kim, T.W., Lee, S.H., Lee, J.H., Lee, H.J., Hong, C.S., Arneborg, L., Björk, G., Kalén, O., 2014. Circulation and modification of warm deep water on the central Amundsen shelf. J. Phys. Oceanogr. 44 (5), 1493–1501.
Haney, J.F., 1988. Diel patterns of zooplankton behavior. Bull. Mar. Sci. 43, 583–603.
Hays, G.C., 2003. A review of the adaptive significance and ecosystem consequences of zooplankton diel vertical migrations. Hydrobiologia 503, 163–170.
Hewitt, R.P., Watkins, J., Naganobu, M., Sushin, V., Brierley, A.S., Demer, D., Kasatkina, S., Takao, Y., Goss, C., Malyshko, A., Brandon, M., Kawaguchi, S., Siegel, V., Trathan, P., Emery, J., Everson, I., Miller, D., 2004. Biomass of Antarctic krill in the Scotia Sea in January/February 2000 and its use in revising an estimate of precautionary yield. Deep-Sea Res. II 51, 1215–1236.
Hubold, G., 1985. On the early life history of the high Antarctic silverfish, *Pleuragramma antarcticum*. In: Siegfried, W.R., Condy, P.R., Laws, R.M. (Eds.), Antarctic Nutrient Cycles and Food Webs. Springer, New York, pp. 445–451.
Hunt, B.P.V., Pakhomov, E.A., Hosie, G.W., Siegel, V., Ward, P., Bernard, K., 2008. Pteropods in Southern Ocean ecosystems. Prog. Oceanogr. 78, 193–221.
Isaacs, J.D., Tont, S.A., Wick, G.L., 1974. Deep scattering layers: vertical migration as a tactic for finding food. Deep-Sea Res. 21, 651–656.
Jacobs, S., Jenkins, A., Hellmer, H., Giulivi, C., Nitsche, F., Huber, B., Guerrero, R., 2012. The Amundsen sea and the Antarctic ice sheet. Oceanography 25, 154–163.
Kampa, E.M., 1970. Underwater daylight and moonlight measurements in the eastern North Atlantic. J. Mar. Biol. Assoc. U. K. 50, 397–420.
Kaneko, A., Koterayama, W., Honji, H., Mizuno, S., Kawatate, K., Gordon, R.L., 1990. Cross-stream survey of the upper 400 m of the Kuroshio by an ADCP on a towed fish. Deep-Sea Res. 37, 875–889.
Kang, S.K., Jung, K.T., Yun, K.D., Lee, K.S., Park, J.S., Kim, E.J., 2012. Tidal dynamics in the strong tidal current environment of the Uldolmok waterway, southwestern tip off the Korean Peninsula. Ocean Sci. J. 47 (4), 453–463.
Kattner, G., Hagen, W., 1998. Lipid metabolism of the Antarctic euphausiid *Euphausia crystallorophias* and its ecological implications. Mar. Ecol. Prog. Ser. 170, 203–213.
La, H.S., Lee, H., Fielding, S., Kang, D., Ha, H.K., Atkinson, A., Park, J., Siegel, V., Lee, S., Shin, H.C., 2015. High density of ice krill (*Euphausia crystallorophias*) in the Amundsen Sea Coastal Polynya, Antarctica. Deep-Sea Res. 95, 75–84.
La Mesa, M., Eastman, J.T., Vacchi, M., 2004. The role of notothenioid fish in the food web of the Ross sea shelf waters: a review. Polar Biol. 27, 321–338.
Lawson, G.L., Wiebe, P.H., Ashjian, C.J., Stanton, T.K., 2008. Euphausiid distribution along the Western Antarctic Peninsula—Part B: distribution of euphausiid aggregations and biomass, and associations with environmental features. Deep-Sea Res. II 55 (3), 432–454.
Lee, R.F., Hagen, W., Kattner, G., 2006. Lipid storage in marine zooplankton. Mar. Ecol. Prog. Ser. 307 (1), 273–306.
Lee, S.H., Kim, B.K., Yun, M.S., Joo, H., Yang, E.J., Kim, Y.N., Shin, H.C., Lee, S., 2012. Spatial distribution of phytoplankton productivity in the Amundsen Sea, Antarctica. Polar Biol. 35 (11), 1721–1733.
Lu, L.G., Liu, J., Yu, F., Wu, W., Yang, X., 2007. Vertical migration of sound scatterers in the southern Yellow Sea in summer. Ocean Sci. J. 42 (1), 1–8.
Madureira, L.S.P., Ward, P., Atkinson, A., 1993. Differences in backscattering strength determined at 120 and 38 kHz for three species of Antarctic macroplankton. Mar. Ecol. Prog. Ser. 93, 17–24.
Nicol, S., 2006. Krill, currents, and sea ice: *Euphausia superba* and its changing environment. BioScience 56, 110–120.
Nordhausen, W., 1994. Distribution and diel vertical migration of the euphausiid *Thysanoessa macrura* in Gerlache Strait, Antarctica. Polar Biol. 14, 219–229.
Orsi, A.H., Whitworth III, T., Nowlin Jr., W.D., 1995. On the meridional extent and fronts of the Antarctic Circumpolar Current. Deep-Sea Res. 42, 641–673.
Perovich, D.K., Roesler, C.S., Pegau, W.S., 1998. Variability in Arctic sea ice optical properties. J. Geophys. Res. 103, 1193–1208.
Plueddemann, A.J., Pinkel, R., 1989. Characterization of the patterns of diel migration using a Doppler sonar. Deep-Sea Res. 36, 509–530.
Pritchard, H.D., Ligtenberg, S.R.M., Fricker, H.A., Vaughan, D.G., van den Broeke, M.R., Padman, L., 2012. Antarctic ice-sheet loss driven by basal melting of ice shelves. Nature 484, 502–505.
Ringelberg, J., 1995. Changes in light intensity and diel vertical migration: a comparison of marine and freshwater environments. J. Mar. Biol. Assoc. U. K. 75, 15–25.
Roe, H.S.J., 1974. Observations on the diurnal vertical migration of an oceanic animal community. Mar. Biol. 28, 99–113.
Schmidt, K., Atkinson, A., Steigenberger, S., Fielding, S., Lindsay, M.C.M., Pond, D.W., Tarling, G.A., Klevjer, T.A., Allen, C.S., Nicol, S., Achterberg, E.P., 2011. Seabed foraging by Antarctic krill: implications for stock assessment, bentho-pelagic coupling, and the vertical transfer of iron. Limnol. Oceanogr. 56 (4), 1411–1428.
Schnack-Schiel, S.B., Hagen, W., Mizdalski, E., 1991. Seasonal comparison of *Calanoides acutus* and *Calanus propinquus* (Copepoda: Calanoida) in the southeastern Weddell Sea, Antarctica. Mar. Ecol. Prog. Ser. 70 (1), 17–27.
Schott, F., 1986. Medium-range vertical acoustic Doppler current profiling from submerged buoys. Deep-Sea Res. 33, 1279–1292.
Shin, C.W., Kim, C., Byun, S.K., Jeon, D.J., Hwang, S.C., 2006. Southwestward intrusion of Korea Strait bottom cold water observed in 2003 and 2004. Ocean Sci. J. 41 (4), 291–299.
Siegel, V., Trathan, P.N., Emery, J., Everson, I., Miller, D.G.M., 2004. Biomass of Antarctic krill in the Scotia Sea in January/February 2000 and its use in revising an estimate of precautionary yield. Deep-Sea Res. II 51, 1215–1236.
Smith Jr., W.O., Ainley, D.G., Cattaneo-Vietti, R., 2007. Trophic interactions within the Ross sea continental shelf ecosystem. Philos. Trans. R. Soc. B 362, 95–111.
Smith, C.R., Demaster, D.J., 2008. Preface and brief synthesis for the FOODBANCS volume. Deep-Sea Res. II 55, 2399–2403.
Stanton, T.K., Chu, D., Wiebe, P.H., Martin, L., Eastwood, R.L., 1998. Sound scattering by several zooplankton groups. I. Experimental determination of dominant scattering mechanisms. J. Acoust. Soc. Am. 103, 225–235.
Steinberg, D.K., Goldthwait, S.A., Hansell, D.A., 2002. Zooplankton vertical migration and the active transport of dissolved organic and inorganic nitrogen in the Sargasso Sea. Deep-Sea Res. 49, 1445–1461.
Thomson, R.E., Allen, S.E., 2000. Time series acoustic observations of macrozooplankton diel migration and associated pelagic fish abundance. Can. J. Fish. Aquat. Sci. 57, 1919–1931.
Thorisson, K., 2006. How are the vertical migrations of copepods controlled? J. Exp. Mar. Biol. Ecol. 329, 86–100.
van Haren, H., 2007. Monthly periodicity in acoustic reflections and vertical motions in the deep ocean. Geophys. Res. Lett. 34 (L12), 603. http://dx.doi.org/10.1029/2007GL029947.
Wade, I.P., Heywood, K.J., 2001. Acoustic backscatter observations of zooplankton abundance and behavior and the influence of oceanic fronts in the northeast Atlantic. Deep-Sea Res. II 48 (2), 899–924.
Wåhlin, A.K., Kalén, O., Arneborg, L., Björk, G., Carvajal, G.K., Ha, H.K., Kim, T.W., Lee, S.H., Lee, J.H., Stranne, C., 2013. Variability of warm deep water inflow in a submarine Trough on the Amundsen Sea Shelf. J. Phys. Oceanogr. 43, 2054–2070.
Wåhlin, A.K., Muench, R.D., Arneborg, L., Björk, G., Ha, H.K., Lee, S.H., Alsén, H., 2012. Some implications of Ekman layer dynamics for cross-shelf exchange in the Amundsen Sea. J. Phys. Oceanogr. 42, 1461–1474.
Wåhlin, A.K., Yuan, X., Björk, G., Nohr, C., 2010. Inflow of warm Circumpolar Deep Water in the central Amundsen shelf. J. Phys. Oceanogr. 40, 1427–1434.
Walker, D.P., Brandon, M.A., Jenkins, A., John, T., Dowdeswell, J.A., Evans, J., 2007. Oceanic heat transport onto the Amundsen Sea shelf through a submarine glacial trough. Geophys. Res. Lett. 34 (L02), 602.
Wallace, M.I., Cottier, F.R., Berge, J., Tarling, G.A., Griffiths, C., Brierley, A.S., 2010. Comparison of zooplankton vertical migration in an ice-free and seasonally ice-covered Arctic fjord: an insight into the influence of sea ice cover on zooplankton behavior. Limnol. Oceanogr. 55 (2), 831–845.
Zaret, T.M., Suffern, J.S., 1976. Vertical migration in zooplankton as a predator avoidance mechanism. Limnol. Oceanogr. 21, 804–813.
Zhou, M., Nordhausen, W., Huntley, M., 1994. ADCP measurements of the distribution and abundance of euphausiids near the Antarctic Peninsula in winter. Deep-Sea Res. 41, 1425–1445.
Zimmerman, R.A., Biggs, D.C., 1999. Patterns of distribution of sound-scattering zooplankton in warm- and cold-core eddies in the Gulf of Mexico from a narrowband acoustic Doppler current profiler survey. J. Geophys. Res. 104 (C3), 5251–5262.